Materials Today Communications 35 (2023) 105574

Contents lists available at ScienceDirect

Materials Today Communications

journal homepage: www.elsevier.com/locate/mtcomm

Sustainable synthesis of SiS_2 for solid-state electrolytes by cascaded metathesis

William H. Smith, Saeed Ahmadi Vaselabadi, Colin A. Wolden *

Chemical and Biological Engineering, Colorado School of Mines, Golden, CO, USA

ARTICLE INFO

Keywords:
Silicon disulfide
Metal sulfide synthesis
Metathesis
Ion exchange
Solid-state electrolyte
Lithium-ion battery

ABSTRACT

Sulfide-based electrolytes containing silicon offer high ionic conductivity and are employed in emerging solid-state batteries that are promising for electric vehicles due to their improved energy density and safety. However, their deployment is constrained by the high cost and low availability of the SiS_2 precursor. Here we introduce a green, solution-based synthesis of SiS_2 through coupled metathesis reactions. First, the key Li_2S precursor is synthesized from the room-temperature reaction between abundant Na_2S and LiCl in ethanol. Next, the Li_2S is recovered from solution and combined with $SiCl_4$ in ethyl acetate to form a SiS_2 solution and regenerate LiCl. The synthesized Li_2S and SiS_2 are characterized and then combined to form a glassy solid electrolyte with a conductivity of 0.11 mS cm^{-1} at 30 °C, validating the utility of metathesis-derived metal sulfides to solid electrolyte synthesis. In this cascaded metathesis scheme the expensive components, LiCl and solvents, are recovered and recycled in a circular economy. The cascaded metathesis process can in principle be used to synthesize nearly any metal sulfide of interest to a wide range of applications including energy conversion/storage, catalysis, electronics, and optics.

1. Introduction

Metal sulfides are a class of compounds with unique chemical, catalytic, electronic, and mechanical properties that make them relevant to a wide range of technological applications. For example, metal sulfides find application as catalysts in the chemical refining industry, industrial lubricants, and light absorbers in solar cells [1–3]. Emerging applications of metal sulfide compounds include electrocatalysts for water splitting, light-emitting devices, and energy storage materials like anodes, cathodes, and solid-state electrolytes [4–6].

The synthesis and preparation of metal sulfides is crucial when precise control over the resulting morphology is required or if the desired compound does not occur naturally. Countless methods to prepare metal sulfide compounds have been developed, such as hydrothermal, chemical vapor deposition, template, and solution-based methods [7]. One such solution-based approach is the metathesis reaction, which has been used to synthesize a wide range of metal sulfide compounds through counter-ion exchange of metal ions with an alkali-metal sulfide salt [4].

Metathesis has been used to form several transition and post-transition metal sulfides (e.g., CdS, ZnS, Ag_2S, PbS, etc.). Traditionally, the metathesis reaction has been conducted by mixing aqueous solutions of a metal sulfide, such as Na_2S, and a water-soluble metal salt (e.g., chlorides, sulfates, nitrates, etc.). Precipitation of the sparingly soluble metal sulfide both drives the reaction and facilitates separation from the resulting salt byproduct, which remains dissolved [8]. Alternately, the metathesis reaction can be conducted in alcohols such as methanol and ethylene glycol or thermally initiated in the absence of solvent and purified by solvent washing after the reaction is complete [9,10].

A key limitation of the traditional metathesis method is the fact that a highly polar protic solvent such as water is generally required to remove the sodium salt byproduct. While water is a good solvent due to its safety and low environmental impact, it limits the scope of metal sulfides that can be synthesized in this manner. For example, important moisture sensitive metal sulfides such as TiS_2 are not accessible using Na_2S metathesis due to their susceptibility for hydrolysis. Additionally, the morphology of the resulting metal sulfides is highly dependent on the properties of the solvent used. Since Na_2S metathesis can be conducted in few solvents, the options for controlling morphology/crystallinity are more limited than if less polar organic solvents can also be considered.

These limitations can be overcome by conducting metathesis with

* Corresponding author.
E-mail address: cwolden@mines.edu (C.A. Wolden).

https://doi.org/10.1016/j.mtcomm.2023.105574
Received 22 December 2022; Received in revised form 3 February 2023; Accepted 7 February 2023
Available online 9 February 2023

Li_2S rather than Na_2S. Li_2S is more reactive in the solid state compared to Na_2S, which improves the reaction when conducted in suspension phase in organic solvents. Furthermore, when Li_2S is used a more covalent salt byproduct such as LiCl forms, which facilitates separation with weakly polar aprotic solvents via dissolution or, as in this work, chloride complexation. The superiority of Li_2S metathesis method was demonstrated by Chianelli and Dines, who explored the synthesis of sulfides of group 4–6 metals – most prominently TiS_2 – using poorly crystalline Li_2S suspended in solvents like THF, EA, and ACN [11]. Pecoraro and Chianelli then extended this synthesis method to the sulfides of group 7–10 metals including MoS_2 for hydrodesulfurization catalysts [12].

Despite the utility of Li_2S as a metathesis reagent, its high cost relative to the resulting metal sulfide and LiCl byproduct constrains implementation of this technique at large scale. However, in a recent publication our group reported the synthesis of Li_2S itself via metathesis from low-cost Na_2S and LiCl in ethanol. The generated Li_2S is recovered from the supernatant by solvent evaporation while the NaCl byproduct is removed as a solid precipitate. Inspired by the work of Chianelli, Dines, and Pecoraro we conceived the Cascaded Metathesis process in which Li_2S is generated in a first metathesis reaction from LiCl and Na_2S, then a metal sulfide is generated in a second metathesis reaction from a metal chloride and Li_2S. The resulting LiCl byproduct, along with the solvents employed, can then be recycled to regenerate the Li_2S intermediate (Fig. 1).

We predict Cascaded Metathesis can be applied in general to a variety of metal sulfide compounds of interest to energy storage/conversion, catalysis, electronics, and optics like those reported in earlier work [11–13]. While the reproduction of these results could be sufficient to demonstrate the concept of Cascaded Metathesis, we instead elected to showcase the flexibility of the process by synthesizing SiS_2, a valuable moisture-sensitive metal sulfide that has not been synthesized from Na_2S/Li_2S metathesis to our knowledge. SiS_2 is of much interest as the preferred precursor for the formation of silicon-based solid-state electrolytes (SSEs) for the fabrication of solid-state lithium-ion batteries with enhanced energy density and improved safety.

In particular, SiS_2 has proven indispensable for glassy SSE formation because it reduces the volatility of high-temperature sulfide melts [14], which allows sulfide glass films to be prepared using a variety of scalable processes such as float casting and melt drawing [15]. For example, a $(Li_2S)_{60}(SiS_2)_{28}(P_2S_5)_{12}$ glass possessing $\sigma_{RT} \sim 2$ mS cm^{-1} and good compatibility with lithium metal anodes was prepared by splat quenching [16]. In the crystalline sulfide SSEs, Si^{4+} serves as a key aliovalent doping cation. For example, the well-known $Li_{9.54}Si_{1.74}P_{1.44}S_{11.7}Cl_{0.3}$ exhibited a σ_{RT} up to 25 mS cm^{-1} [17,18].

Despite the high abundance and low cost of its constituent elements, SiS_2 is currently prohibitively expensive (estimated >1000 USD kg^{-1} at the ton scale, see Table S1, Fig. S1) and available from just a few vendors. The high cost and low availability of SiS_2 reflects the difficulty of synthesis, which relies either on high-temperature reactions lasting days or hazardous and expensive reagents and reaction conditions. For example, the reaction between Si and S is conducted by heating the mixed reagents at 800 – 1100 °C for several hours or more and is limited to sealed ampoule heating due to the high volatility of sulfur at these temperatures [19,20]. Other, more scalable methods rely on the reaction of a silicon precursor with hazardous H_2S or CS_2 gas at 1000 – 1500 °C to form SiS gas, which subsequently decomposes to form SiS_2 solid crystals and S_2 gas [21]. These and other common synthesis methods are summarized in Table 1.

In this work, we demonstrate the utility of Cascaded Metathesis for the synthesis of SiS_2. We first show that the synthesis of SiS_2 from Na_2S and $SiCl_4$ is constrained by the low reactivity of Na_2S and challenges of separating the NaCl byproduct. Next, we demonstrate that complete conversion of Li_2S to SiS_2 can be achieved when reacting with $SiCl_4$ in polar aprotic solvents like ethyl acetate. SiS_2 can be partially separated from the solid LiCl byproduct by chloride complexation and recovered from the reaction supernatant with solvent evaporation. Finally, the LiCl is recovered and reacted once again with fresh Na_2S to reform the Li_2S intermediate, reducing the need for lithium by ~95% and demonstrating the validity of solvent recycling. The synthesized SiS_2 and Li_2S are used to fabricate the binary $60Li_2S•40SiS_2$ glass via high-energy ball milling, exhibiting $\sigma_{30} = 0.11$ mS cm^{-1} in good agreement with literature reports.

2. Materials and methods

2.1. Materials

Technical grade Na_2S hydrate (≥60%, Sigma) was purified as described previously [25]. In brief, the material was ground and dried at 70–150 °C for 12 h under vacuum, then annealed at 600 °C under flowing 50% H_2/Ar in a custom-built tubular reactor for 12 h. LiCl (99%, Sigma) was ground and dried at 150 °C under vacuum for 12 h. Li_2S (99.9%, Alfa), $SiCl_4$ (99.998%, Sigma), EA (anhydrous, 99.8%, Sigma), tetrahydrofuran (THF, unstabilized, 99%, Alfa), EtOH (anhydrous, 99.5%, Sigma), acetonitrile (ACN, anhydrous, 99.8%, Alfa), 1,2-dimethoxyethane (DME, stabilized, 99%, Alfa), n-butyl acetate (99%, Alfa), P_2S_5 (98%, Sigma), silicon (98%, Alfa), sulfur (99.5%, Alfa), and Ar

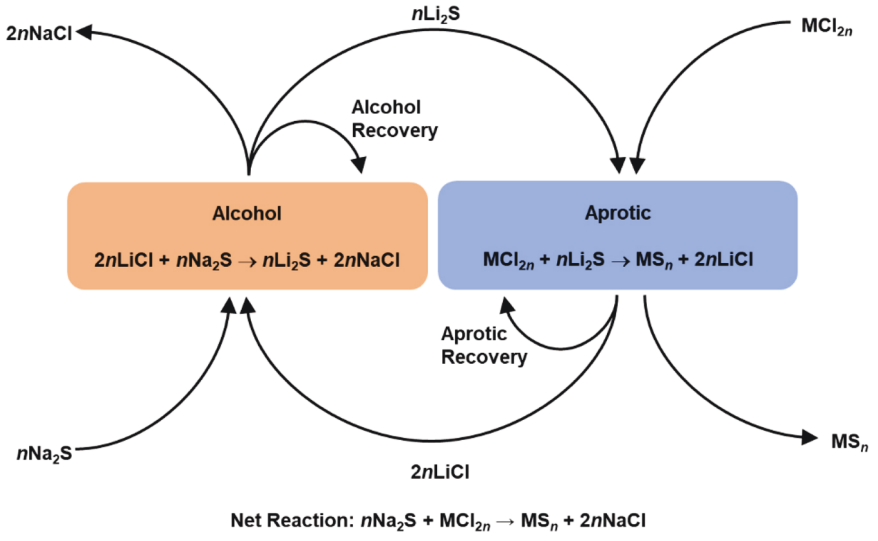

Fig. 1. Schematic of the cascaded metathesis process.

Table 1
SiS_2 Synthesis Methods.

#	Title	Reaction (s)	Notes	Reference
1	Elemental Reaction	$Si + 2S \rightarrow SiS_2$	1100 °C for up to 3 d Preliminary sulfur coating allows temperature reduction to 800 °C Limited to ampoule reaction	[19,20, 22]
2	Gas-Phase Sulfurization	$Si + CS_2 \rightarrow SiS_2 + C$ $Si + 2\ H_2S \rightarrow SiS_2 + 2\ H_2$	1000 – 1500 °C Hazardous sulfide gases Manual separation of SiS_2 crystal from solid byproducts	[21,23]
3	Al_2S_3 Sulfurization	$3SiO_2 + 2Al_2S_3 \rightarrow 3SiS_2 + 2Al_2O_3$	1250 °C Expensive Al_2S_3 Separation of products via SiS_2 sublimation at 1200 °C	[24]
4	Silicide Reduction	$M_xSi_y + 2yS \rightarrow ySiS_2 + xM$ (M = magnesium, calcium, etc.)	Expensive silicides Extremely exothermic/explosive	[23]
5	Organosilicon Decomposition	$Si(SC_2H_5)_4 + 2S \rightarrow SiS_2 + 2(SC_2H_5)_2$	200 – 300 °C Expensive organosilicon precursors	[23]
6	Metathesis	$2\ M_2S + SiCl_4 \rightarrow SiS_2 + 4MCl$ M = Li or Na	Room temperature, ~1 atm, ethyl acetate Li preferred due to reactivity/separation	This work

(99.999%, General Air) were used as-received without purification. Some Li_2S/Na_2S was ball-milled for 2 h to reduce particle size.

2.2. Synthesis

SiS_2 was synthesized by suspending 0.67 g of Na_2S or 0.40 g of Li_2S in 40 mL of solvent (either EA, THF, ACN, or DME) for 30 min. Next, 1.1x stoichiometric mass of $SiCl_4$ was added to the suspension, then stirred for 12 h. Then, the product suspension was centrifuged at 4000 rpm for 30 min and decanted. The precipitate was dried at 100 °C under vacuum for 2 h. The supernatant was evaporated at 100 °C under vacuum with stirring for 2 h. Li_2S was synthesized as described previously [26]. In brief, LiCl was dissolved in EtOH at 1.8 M, then Na_2S was added with stirring. The suspension was stirred for 12 h, then centrifuged at 4000 rpm for 30 min. The supernatant was decanted and evaporated under vacuum at 100 °C with stirring for 2 h to yield a solid Li_2S-EtOH complex that was further dried at 300 °C for 12 h under flowing Ar in a custom-built fluidized-bed dryer. In the solvent evaporation steps, solvent was recovered in a condenser maintained at ~0 °C in an ice bath. Solvent recovery was generally ~80%. A second reaction cycle was conducted for Li_2S in EA using recycled solvents and LiCl at 80% of the scale indicated above. The $60Li_2S•40SiS_2$ glassy electrolyte was synthesized by mixing 0.5 g total of metathesis-derived Li_2S and SiS_2 by mortar and pestle followed by ball-milling in a sealed ZrO_2 jar (40 mL) with 3 ZrO_2 balls (10 mm diameter) for a total of 20 h in 2 h increments with 1 h rest in between to allow heat to dissipate. 10% excess SiS_2 was added to account for the LiCl content of the material. Synthesis steps were carried out under Ar in a dry glove box.

2.3. Characterization

X-ray diffraction (XRD) was measured on a Philips X'Pert X-ray diffractometer with Cu Kα radiation (λ = 0.15405 nm) between 10° and 70° at a scan rate of 2° min^{-1} (step size = 0.05°). Samples were prepared on a glass slide with a piece of Scotch Magic Tape covering the material to prevent undesired reactions with ambient moisture. The contribution from the quartz slide was background subtracted with a polynomial fit. Fourier-transform infrared spectroscopy (FTIR) was performed with a Nicolet Summit FTIR spectrometer using an attenuated total reflection (ATR) accessory equipped with a diamond crystal. Field emission scanning electron microscopy (FESEM) images were taken on a JEOL JSM-7000 F FESEM instrument with an accelerating voltage of 15 kV. Energy-Dispersive Analysis of X-rays (EDAX) was performed on the same instrument at 15 kV. Quantification of Si, S, and Cl was standardized by measuring a standard in the same session under the same conditions as the experimental sample. The standard was prepared by ball-milling 1.0 g total of Si (27.4 wt%), S (62.6 wt%), and LiCl (10.0 wt%) for 2 h to ensure homogeneity. Mass percentages were normalized to lithium-free mass, and resulting unknown concentrations were adjusted assuming all Cl exists as LiCl. Electrochemical impedance spectroscopy (EIS) was performed in the frequency range of 1 Hz to 1 MHz with a 10 mV perturbation on a pelletized electrolyte sample. The sample was pelletized by pressing 0.25 g into a 12 mm diameter pellet in a PEEK split cell with stainless steel plungers under a uniaxial fabrication pressure of 320 MPa and held for 2 min. The pressure was released for 1 min, then increased again to 120 MPa for electrical testing. Temperature during testing was controlled by an electrical heating element allowed to stabilize for 1 h. The accuracy of the temperature control was verified by measuring the surface temperature of the sample with a thermocouple inserted in the split cell. The ionic resistance was calculated by regressing a linear fit of the capacitive spike to the Z_{re}-intercept on the Nyquist plot.

3. Results and discussion

The direct reaction between Na_2S and $SiCl_4$ in either THF or EA was first explored. However, the reaction did not proceed in THF and only to a limited extent in EA. (Fig. S2) Moreover, despite ball-milling the Na_2S to enhance its reactivity, the reaction did not proceed to completion, and second, no separation of SiS_2/NaCl was provided. These observations are in good agreement with literature reports that noted the poor reactivity of Na_2S in the solid state, and the difficulty of separating NaCl and moisture-sensitive metal sulfides. To overcome these limitations, we next investigated the use of Li_2S as the sulfide reagent rather than Na_2S.

Originally, it was expected that THF would be the ideal solvent for the SiS_2 reaction as it was for the synthesis of TiS_2 since it was predicted to have good chemical compatibility and high solubility for LiCl. However, when commercial Li_2S (Li_2S-c) was reacted with $SiCl_4$ in THF, almost all of the material dissolved, leaving behind residual unreacted Li_2S in the solid state. When the supernatant was evaporated, a waxy material containing LiCl and chlorinated solvent byproduct was recovered (Fig. S3). For this reason, the less polar EA was investigated.

Due to the low solubility of LiCl and SiS_2 in EA, it was expected that a solid product consisting of both LiCl and SiS_2 would be recovered from the reaction precipitate as was observed when using Na_2S as the sulfide reagent. However, when using Li_2S as the reagent, it was found that SiS_2 could be recovered from the supernatant rather than the precipitate. When Li_2S-c was used as-received (without milling), incomplete reaction was achieved, resulting in a mixture of Li_2S and LiCl in the precipitate in the form of a white powder. However, ball-milling the Li_2S-c for 2 h enhanced its reactivity, resulting in only detection of the LiCl byproduct in the precipitate with 90% yield (Fig. 2-a). A beige powder recovered from the supernatant contained crystalline LiCl and poorly crystalline SiS_2 in either case, with 96% yield when using ball-milled Li_2S (Fig. 2-b). FTIR of the supernatant in either case showed three significant peaks at 477, 582, and 1085 cm^{-1}, which are attributed to Si-S-Si rocking, bond-bending, and stretching vibrational modes, respectively. The peak locations and relative intensities are in good agreement with the spectrum of high-purity SiS_2 reported in the literature [27]. Alternative solvents, including ACN and DME, were tested to explore the impact of different solvent chemistries on the synthesis of SiS_2. The

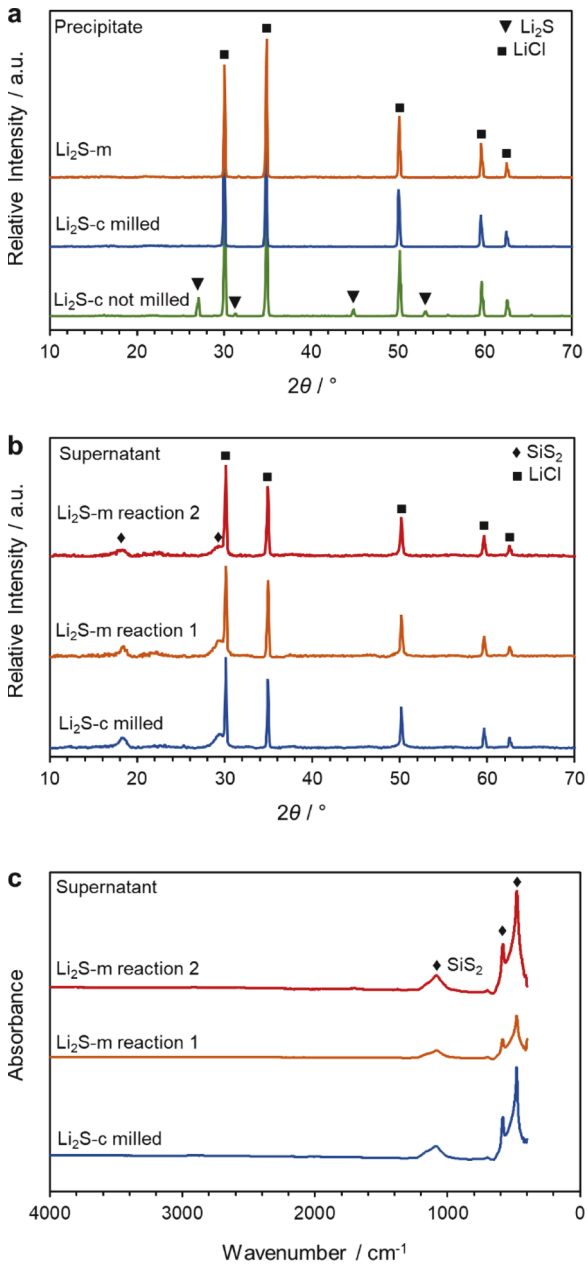

Fig. 2. Suspension reaction between Li_2S and $SiCl_4$ in EA with different Li_2S reagents. a) XRD of the precipitate, b) XRD, and c) FTIR of material recovered from the supernatant.

synthesis was apparently successful in either solvent, resulting in similar yields of LiCl in the precipitate and LiCl-contaminated material in the supernatant. While FTIR shows the same Si-S-Si bonding for both, XRD shows the SiS_2 is much less crystalline than that obtained from EA (Fig. S4).

Despite the ability of Li_2S to react completely with $SiCl_4$ and effectively partition the chloride and sulfide products into the solid and liquid state, respectively, the cost benefits of using Na_2S instead are undeniable (<1 USD kg^{-1} for Na_2S [28] compared to >700 USD kg^{-1} for Li_2S [29]). In a recent publication, we reported the synthesis of Li_2S by metathesis of Na_2S and LiCl [26]. This metathesis reaction is conducted in solution in EtOH, with precipitation of sparingly soluble NaCl occurring spontaneously at room temperature and pressure. The Li_2S is then recovered from the supernatant via solvent evaporation followed by annealing at 300 °C to remove residual solvent. An overview of the Li_2S metathesis, including images of the reaction steps and XRD of the material, is included in the Supporting Information (Fig. S5). Given the high recovery of LiCl in the SiS_2 synthesis, we were inspired to synthesize SiS_2 from metathesis-derived Li_2S (Li_2S-m), then recycle the LiCl byproduct to repeat the sequential metathesis reactions. In this Cascaded Metathesis process, net consumption of lithium may be reduced greatly, and the synthesis no longer relies on expensive Li_2S, but instead on low-cost, abundant Na_2S.

First, Li_2S-m was synthesized from fresh LiCl via metathesis with Na_2S (Fig. S5-f, "Reaction 1"). Next, the Li_2S-m was employed in the metathesis reaction with $SiCl_4$ in EA. The precipitate consisted only of LiCl, indicating that full conversion of Li_2S-m can be achieved without ball-milling, with 95% yield (Fig. 2-a). SiS_2 was obtained from the supernatant at 70% yield and displays a nearly identical XRD pattern and FTIR spectrum compared to SiS_2 formed from ball milled Li_2S-c (Fig. 2-b, c, "Reaction 1"). The solvents used in either reaction (EtOH and EA) were recovered via condensation and recycled for use in the second reaction cycle. FTIR of the recovered solvents are reported in the Supporting Information alongside spectra of the neat solvents, demonstrating that no decomposition occurred during reaction/evaporation. (Fig. S6) Next, the LiCl obtained from the precipitate was reacted with Na_2S in recycled EtOH to form Li_2S-m. XRD indicates nearly phase-pure Li_2S is formed comparable to that synthesized with fresh LiCl (Fig. S5-f, "Reaction 2"). A minor NaHS phase attributed to the alcoholysis of residual unreacted Na_2S was detected, indicating further purification of the LiCl byproduct may be beneficial. However, the impurity apparently has little impact on the subsequent metathesis, which produced SiS_2 with XRD pattern and FTIR spectrum nearly identical to that generated in the first reaction cycle (Fig. 2-b, c, "Reaction 2").

The mechanism of SiS_2 dissolution is not fully understood, and it contrasts with the Na_2S reaction in which the generated SiS_2 remained undissolved. Recently, it was reported that SiS_2 has good solubility in ACN when mixed with Li_2S in a molar ratio of 2:1 [30]. However, in this work, essentially all of the Li_2S is consumed, as evidenced by the near quantitative recovery of LiCl. Alternatively, metal polysulfides are well known to have higher solubility than the sulfides [31], but elemental analysis indicates no excess sulfur is present (see below). Li et al. reported the dissolution of GeS_2 in a mixture of 1,2-ethylenediamine (EDA):1,2-ethanedithiol(EDT) by Ge-S bond breaking due to nucleophilic attack of thiolate anions formed via the deprotonation of EDT by EDA [32]. Similarly, P_2S_5 could be dissolved in THF by addition of 1 mol lithium thiolate ($LiSC_2H_5$) per mol P_2S_5 via P-S bond breaking due to nucleophilic attack on the P^{5+} cation [33]. In the SiS_2 formed in this work, we hypothesize that dissolved LiCl, due to the nonzero solubility in EA of about 0.03 M, has a solubilizing effect. LiCl is commonly used in organic synthesis to generate Cl^- anions in organic solvents to serve as a nucleophile and ligand [34]. By analogy with the previous examples of dissolution via nucleophilic attack, we suggest that neutral SiS_2 is converted to a more soluble intermediate by nucleophilic attack of dissolved Cl^- at the Si^{4+} cation according to the following: $Li^+ + Cl^- + SiS_2 \rightarrow Li^+ + [SiS_2Cl]^-$. Decomposition of this soluble chloride complex into the more stable LiCl and SiS_2 presumably occurs during the solvent evaporation process.

Given the key role of LiCl in solubilizing the SiS_2, quantification of the LiCl concentration in the final material is key. Elemental analysis was performed by EDAX (see Experimental Section for details) (Fig. 3-a). The composition of the synthesized material can be expressed as $SiS_x \bullet yLiCl$. By EDAX, $x \geq 1.5$ and $y = 0.7$. While x is below the expected value of 2, it should be noted that substitution of S for O occurs during the transfer under air into the SEM chamber. This is reflected in the high O peak in EDAX of the experimental sample compared to the that of the standard composed of Si, S, and LiCl with $x = 2$ and $y = 0.226$ (w_{LiCl} = 10 wt%) (Fig. S7). Therefore, it is argued that the S:Si ratio is at minimum 1.5, and likely closer to the stoichiometric value of 2. Assuming this to be the case, the ratio of LiCl:Si is equivalent to a LiCl concentration ≈ 25 wt%. A simple comparison of the x-ray diffractograms of the material from the precipitate and supernatant (Fig. 3-b) shows the

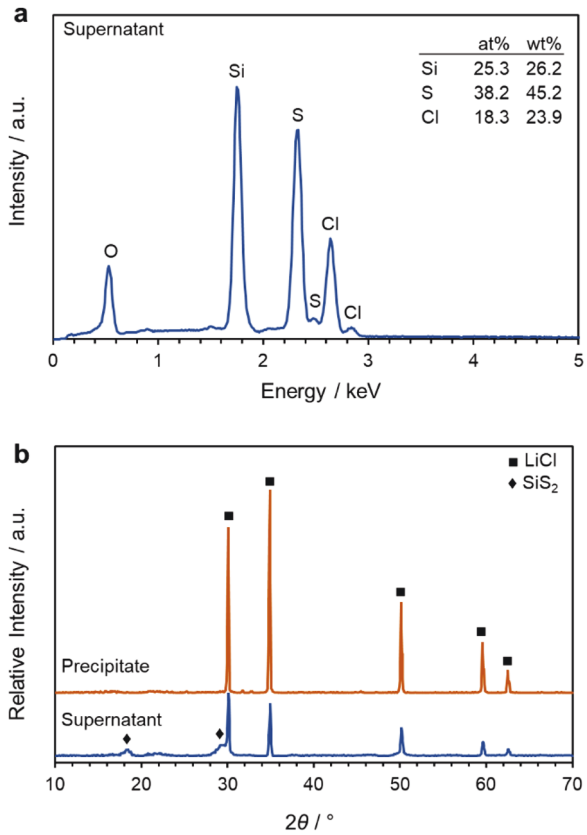

Fig. 3. a) EDAX of SiS_2 recovered from the EA reaction supernatant with elemental composition adjusted for Li content (inset). b) XRD comparison of supernatant and precipitate materials.

LiCl peaks in the supernatant are attenuated by a factor of about 4, which is consistent with the above value of 25 wt%.

The morphology of the SiS_2 and LiCl products was investigated by SEM (Fig. 4). The SiS_2 consists of large irregular granules of non-uniform shape and size up to 300 μm. The surface of the granules is smooth with little porosity or underlying grain structure visible, reflecting the glass-like quality of the material. On the other hand, the LiCl consists of regular crystals with a much more uniformly distributed size of 10–20 μm, reflecting the high purity and crystallinity of LiCl recovered from the precipitate. Additional images at different magnifications showing the particle uniformity, as well as the surface of a SiS_2 particle, are provided in Fig. S8.

Finally, to validate the use of the synthesized SiS_2 as a SSE precursor, a model glassy electrolyte – $60Li_2S•40SiS_2$ – was prepared from metathesis-derived sulfides via high-energy ball milling. XRD of the material before and after ball-milling verifies the amorphization of the initial crystalline phases, namely Li_2S and LiCl present in the SiS_2 material (Fig. 5-a). Electrochemical impedance spectroscopy (Fig. 5-b) was performed on a pelletized sample of the glass at varying temperatures to measure the ionic conductivity and extract an activation energy from the resulting Arrhenius plot (Fig. 5-c). The ionic conductivity at 30 °C was 0.11 mS cm^{-1} in good agreement with literature reports [35,36]. However, the activation energy was 20.2 kJ mol^{-1}, which is significantly lower than the value of 30 kJ mol^{-1} that is typically reported for these materials. We suggest that the lower activation energy may be attributed to a slight sulfur deficiency in the SiS_2 (see EDAX above). Alternatively, the deviation could be attributed to the amorphous nature of the SiS_2, which could impact the resulting energy landscape of the SSE. The presence of LiCl is unlikely to cause this effect since the ionic conduction in $50Li_2S•50SiS_2$ glasses was found to be nearly insensitive to LiCl concentrations up to 40 mol% [35].

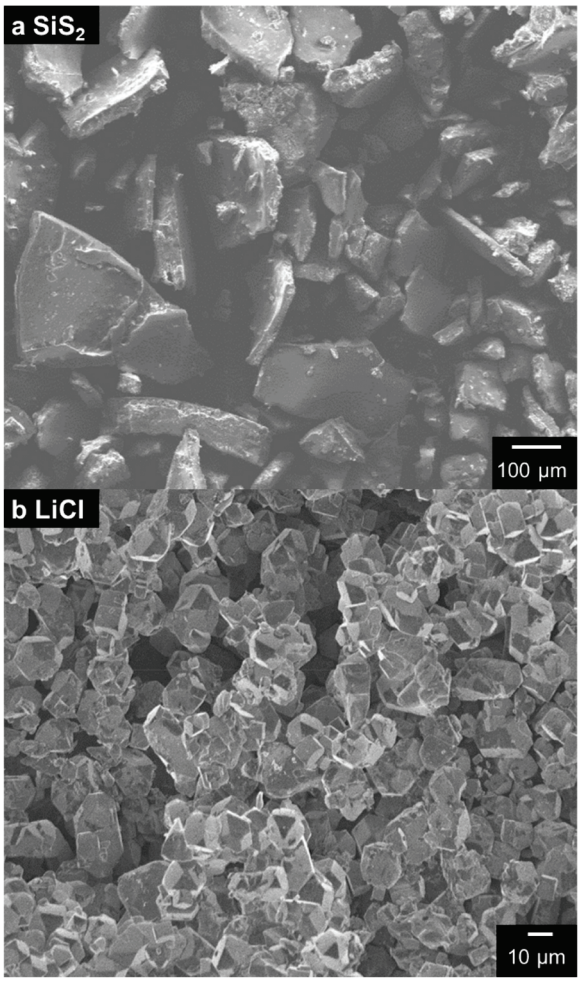

Fig. 4. SEM images of a) SiS_2 and b) LiCl from ethyl acetate.

4. Conclusions

Metal sulfide compounds are of great interest in several emerging technological applications. However, advanced synthesis and processing methods are needed to produce metal sulfides at large scale with the desired properties for their intended applications. Metathesis is an elegant and easily scalable synthesis approach that can meet these requirements. Here, we introduce Cascaded Metathesis and demonstrated it by synthesizing SiS_2 – a key precursor for the fabrication of silicon-based sulfide solid-state electrolytes – via metathesis of alkali-metal sulfides Na_2S and Li_2S with $SiCl_4$ in organic solvents such as ethyl acetate. We showed that Li_2S is the preferred sulfide reagent due to its higher reactivity compared to Na_2S and the ability of the LiCl byproduct to solubilize the SiS_2. The SiS_2 produced in this manner was poorly crystalline but exhibited characteristic Si-S-Si vibrational modes in FTIR. Furthermore, EDAX indicated the material was composed of nearly stoichiometric SiS_2 with a LiCl content of about 25 wt%. Low-cost Li_2S derived from metathesis of Na_2S and LiCl in ethanol was utilized in the synthesis of SiS_2, exhibiting superior reactivity to a commercial Li_2S sample. 95% of the LiCl byproduct was recovered, and the solvents showed no evidence of decomposition. Therefore, the LiCl and solvents were recycled to be reused in a second reaction cycle that resulted in nearly identical Li_2S and SiS_2 according to XRD and FTIR. Finally, the metathesis-derived SiS_2 and Li_2S were employed as precursors in the synthesis of a glassy electrolyte that exhibited a conductivity of 0.11 mS cm^{-1} at 30 °C with a low activation energy of 20.2 kJ mol^{-1}, validating the promise of Cascaded Metathesis for the synthesis of metal sulfide compounds for solid-state electrolytes. In future studies, this new

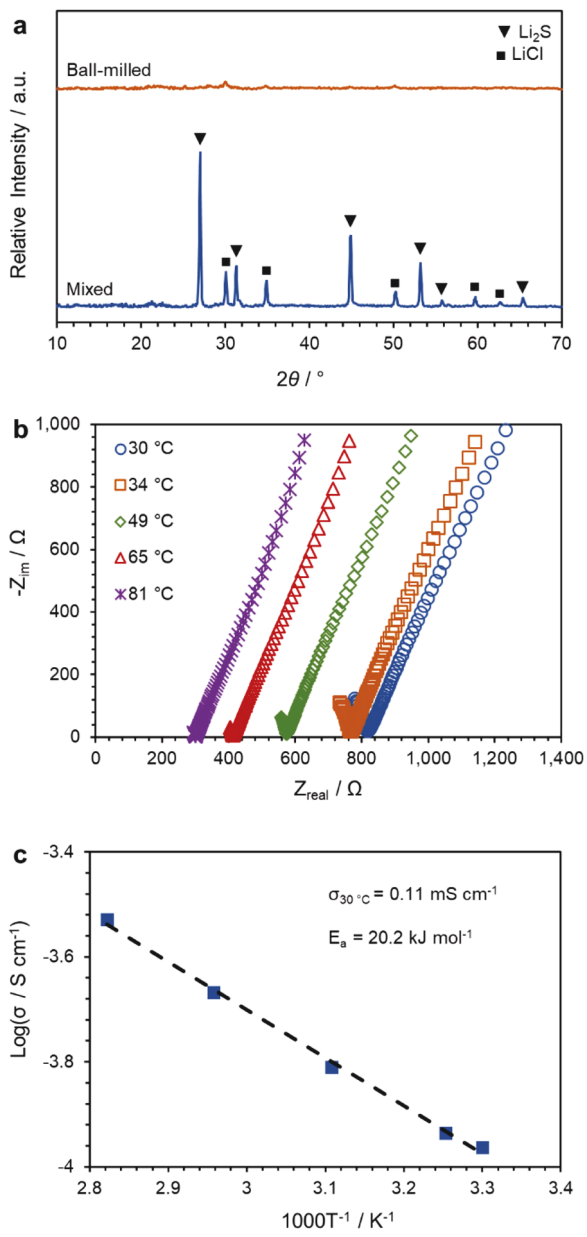

Fig. 5. a) XRD, b) EIS, and c) Arrhenius plot of the 60Li2S•40SiS_2 glassy electrolyte.

metathesis approach will be leveraged to synthesize compounds in the Li_2S-SiS_2-P_2S_5-LiCl system.

CRediT authorship contribution statement

William Smith: Conceptualization, Methodology, Investigation, Writing – original draft preparation. **Saeed Ahmadi Vaselabadi:** Investigation. **Colin Wolden**: Supervision, Funding acquisition, Writing – review & editing.

Declaration of Competing Interest

The authors declare the following financial interests/personal relationships which may be considered as potential competing interests: Colin A. Wolden reports financial support was provided by National Science Foundation. Colin A. Wolden and William H. Smith have a patent METHOD OF MAKING ANHYDROUS METAL SULFIDE NANOCRYSTALS pending to Colorado School of Mines.

Data availability

Data will be made available on request.

Acknowledgements

This work was supported by the National Science Foundation through Awards 1825470 and 2219184 the Colorado Office of Economic Development and International Trade, and Solid Power.

Supporting Information

SiS_2 pricing information and additional characterization of materials/solvents.

Appendix A. Supporting information

Supplementary data associated with this article can be found in the online version at doi:10.1016/j.mtcomm.2023.105574.

References

[1] R.R. Chianelli, G. Berhault, B. Torres, Unsupported transition metal sulfide catalysts: 100 years of science and application, Catal. Today 147 (3–4) (2009) 275–286.
[2] V.N. Bakunin, A.Y. Suslov, G.N. Kuzmina, O.P. Parenago, A.V. Topchiev, Synthesis and application of inorganic nanoparticles as lubricant components – a review, J. Nanopart. Res. 6 (2/3) (2004) 273–284.
[3] D.G. Moon, S. Rehan, D.H. Yeon, S.M. Lee, S.J. Park, S. Ahn, Y.S. Cho, A review on binary metal sulfide heterojunction solar cells, Sol. Energy Mater. Sol. Cells (2019) *200*.
[4] S. Chandrasekaran, L. Yao, L. Deng, C. Bowen, Y. Zhang, S. Chen, Z. Lin, F. Peng, P. Zhang, Recent advances in metal sulfides: from controlled fabrication to electrocatalytic, photocatalytic and photoelectrochemical water splitting and beyond, Chem. Soc. Rev. 48 (15) (2019) 4178–4280.
[5] W. Zhu, K. Ding, C. Yi, R. Chen, B. Wei, L. Huang, J. Li, Use of Hybrid PEDOT:PSS/Metal Sulfide Quantum Dots for a Hole Injection Layer in Highly Efficient Green Phosphorescent Organic Light-Emitting Diodes, Front Chem. 9 (2021), 657557.
[6] X. Xu, W. Liu, Y. Kim, J. Cho, Nanostructured transition metal sulfides for lithium ion batteries: Progress and challenges, Nano Today 9 (5) (2014) 604–630.
[7] Y. Liu, Y. Li, H. Kang, T. Jin, L. Jiao, Design, synthesis, and energy-related applications of metal sulfides, Mater. Horiz. 3 (5) (2016) 402–421.
[8] H. Estay, L. Barros, E. Troncoso, Metal sulfide precipitation: recent breakthroughs and future outlooks, Minerals 11 (12) (2021) 1385.
[9] I.P. Parkin, Solid state metathesis reaction for metal borides, silicides, pnictides and chalcogenides: ionic or elemental pathways, Chem. Soc. Rev. 3 (1996) 199–207.
[10] K. Li, S. Yan, Z. Lin, Y. Shi, Facile solution synthesis of tin sulfide nanobelts for lithium-ion batteries, J. Alloy. Compd. 681 (2016) 486–491.
[11] R.R. Chianelli, M.B. Dines, Low-temperature solution preparation of group 4B, 5B and 6B transition-metal dichalcogenides, Inorg. Chem. 17 (10) (1978) 2758–2762.
[12] T. Pecoraro, R.R. Chianelli, Hydrodesulfurization catalysis by transition metal sulfides, J. Catal. 67 (2) (1981) 430–445.
[13] R.R. Chianelli, E.B. Prestridge, T.A. Pecoraro, J.P. Deneufville, Molybdenum disulfide in the poorly crystalline "Rag" structure, Science 203 (4385) (1979) 1105–1107.
[14] R. Zhao, S. Kmiec, G. Hu, S.W. Martin, Lithium Thiosilicophosphate Glassy Solid Electrolytes Synthesized by High-Energy Ball-Milling and Melt-Quenching: Improved Suppression of Lithium Dendrite Growth by Si Doping, ACS Appl. Mater. Interfaces 12 (2) (2020) 2327–2337.
[15] S.J. Visco, Y.S.D. Nimon, L.C. De Jonghe, B.D. Katz, V. Nimon, Vitreous solid electrolyte sheets of Li ion conducting sulfur-based glass and associated structures, Cells Methods EP 3 (227 952 B1) (2017).
[16] T.A. Yersak, J.R. Salvador, N.P.W. Pieczonka, M. Cai, Dense, Melt Cast Sulfide Glass Electrolyte Separators for Li Metal Batteries, J. Electrochem. Soc. 166 (8) (2019) A1535–A1542.
[17] Y. Kato, S. Hori, T. Saito, K. Suzuki, M. Hirayama, A. Mitsui, M. Yonemura, H. Iba, R. Kanno, High-power all-solid-state batteries using sulfide superionic conductors, Nat. Energy 1 (4) (2016) 16030.
[18] S. Harm, A.-K. Hatz, I. Moudrakovski, R. Eger, A. Kuhn, C. Hoch, B.V. Lotsch, Lesson Learned from NMR: Characterization and Ionic Conductivity of LGPS-like Li7SiPS8, Chem. Mater. 31 (4) (2019) 1280–1288.
[19] M. Tenhover, M.A. Hazle, R.K. Grasselli, Atomic Structure of SiS2 and SiSe2 Glasses, Phys. Rev. Lett. 51 (5) (1983) 404–406.
[20] M.-X. Xie, J.-W. Zhang, Y. Zhang, H.-R. Wu, Y.-P. Wang, W.-H. Wang, G.-Q. Shao, Synthesis and growth mechanism of SiS_2 rods, ACS Omega 7 (26) (2022) 22500–22510.

[21] R.O. Suzuki, Y. Yashima, T. Kaneko, E. Ahmadi, T. Kikuchi, T. Watanabe, G. Nogami, Synthesis of Silicon Sulfide by Using CS2 Gas, Metall. Mater. Trans. B 52 (3) (2021) 1379–1391.
[22] Y. Zhang, M.-X. Xie, W. Zhang, J.-L. Yan, G.-Q. Shao, Synthesis and purification of SiS_2 and Li_2S for $Li_{9.54}Si_{1.74}P_{1.44}S_{11.7}Cl_{0.3}$ solid electrolyte in lithium-ion batteries, Mater. Lett. 266 (2020), 127508.
[23] A. Haas, The Chemistry of Silicon-Sulfur Compounds, Angew. Chem., Int. Ed. Engl. 4 (12) (1965) 1014–1023.
[24] I. Tomaszkiewicz, G.A. Hope, P.A.G. O'Hare, A fluorine bomb calorimetric determination of the standard molar enthalpy of formation of silicon disulfide SiS2 (cr) at the temperature 298.15 K. Enthalpies of dissociation of Si-S bonds, J. Chem. Thermodyn. 29 (9) (1997) 1031–1045.
[25] W.H. Smith, J. Birnbaum, C.A. Wolden, Production and purification of anhydrous sodium sulfide, J. Sulfur Chem. (2021) 1–17.
[26] W.H. Smith, S.A. Vaselabadi, C.A. Wolden, Argyrodite superionic conductors fabricated from metathesis-derived Li_2S, ACS Appl. Energy Mater. 5 (4) (2022) 4029–4035.
[27] J.H. Kennedy, Y. Yang, Glass-Forming Region and Structure in SiS2-Li2S-LiX (X = Br, I), J. Solid State Chem. 69 (1987) 252–257.
[28] F. Trausel, A.-J. De Jong, R. Cuypers, A review on the properties of salt hydrates for thermochemical storage, Energy Procedia 48 (2014) 447–452.
[29] H. Kwak, S. Wang, J. Park, Y. Liu, K.T. Kim, Y. Choi, Y. Mo, Y.S. Jung, Emerging halide superionic conductors for all-solid-state batteries: design, synthesis, and practical applications, ACS Energy Lett. 7 (5) (2022) 1776–1805.
[30] T. Ito, S. Hori, M. Hirayama, R. Kanno, Liquid-phase synthesis of the Li10GeP2S12-type phase in the Li–Si–P–S–Cl system, J. Mater. Chem. A 10 (27) (2022) 14392–14398.
[31] A. Müller, E. Diemann, Polysulfide complexes of metals, *Adv. Inorg. Chem.* (1987) 89–122.
[32] J.E. Lee, K.H. Park, J.C. Kim, T.U. Wi, A.R. Ha, Y.B. Song, D.Y. Oh, J. Woo, S. H. Kweon, S.J. Yeom, W. Cho, K. Kim, H.W. Lee, S.K. Kwak, Y.S. Jung, Universal solution synthesis of sulfide solid electrolytes using alkahest for all-solid-state batteries, Adv. Mater. 34 (16) (2022), 2200083.
[33] H.-D. Lim, X. Yue, X. Xing, V. Petrova, M. Gonzalez, H. Liu, P. Liu, Designing solution chemistries for the low-temperature synthesis of sulfide-based solid electrolytes, J. Mater. Chem. A 6 (17) (2018) 7370–7374.
[34] J.S. Nowick, G. Lutterbach, J.K. Barbay, W. He, Encyclopedia of Reagents for Organic Synthesis, John Wildey & Sons,, 2001.
[35] J.H. Kennedy, S. Sahami, S.W. Shea, Z. Zhang, Preparation and Conductivity Measurements of SiS2-Li2S Glasses Doped with LiBr and LiCI, Solid State Ion. 18–19 (1986) 368–371.
[36] H. Morimoto, H. Yamashita, M. Tatsumisago, T. Minami, Mechanochemical synthesis of new amorphous materials of 60Li2S·40SiS2 with high lithium ion conductivity, J. Am. Ceram. Soc. 82 (5) (2004) 1352–1354.